New Magic Number, $N = 16$, near the Neutron Drip Line

A. Ozawa,[1] T. Kobayashi,[2] T. Suzuki,[3] K. Yoshida,[1] and I. Tanihata[1]

[1]*The Institute of Physical and Chemical Research (RIKEN), Hirosawa 2-1, Wako-shi, Saitama 351-0198, Japan*

[2]*Department of Physics, Tohoku University, Miyagi 980-8578, Japan*

[3]*Department of Physics, Niigata University, Niigata 950-2181, Japan*

(Received 15 February 2000)

We have surveyed the neutron separation energies (S_n) and the interaction cross sections (σ_I) for the neutron-rich *p-sd* and the *sd* shell region. Very recently, both measurements reached up to the neutron drip line, or close to the drip line, for nuclei of $Z \leq 8$. A neutron-number dependence of S_n shows clear breaks at $N = 16$ near the neutron drip line ($T_Z \geq 3$), which shows the creation of a new magic number. A neutron-number dependence of σ_I shows a large increase of σ_I for $N = 15$, which supports the new magic number. The origin of the new magic number is also discussed.

PACS numbers: 21.10.Dr, 21.10.Pc, 25.60.Dz, 27.30.+t

Recently, nuclear structure for neutron-rich nuclei has attracted much attention because of its exotic nature, such as a halo and a skip [1]. However, experimental observations have been limited to neutron-rich nuclei due to access difficulties. Recent improvements of secondary-beam techniques now allow us to measure the mass and the interaction cross sections (σ_I) for nuclei on the neutron drip line or close to the drip line. Direct mass measurements have reached or been near the drip line for $Z \leq 8$ [2]. On the other hand, measurements of σ_I have reached the drip line for $Z \leq 8$, except for ^{22}C [3]. Both improvements allow us to survey the systematics of neutron separation energies (S_n) and σ_I for the neutron-rich *p-sd* and the *sd* shell region. It is noted that recent progress involving a Glauber model analysis for σ_I allows us to distinguish the angular momentum of a valence neutron and provides some spectroscopic information [3]. The analysis is a good tool to investigate nuclear structure for neutron-rich nuclei, where spectroscopic information, even for spin parity, is not known at all.

The shell structure is one of the very important quantities concerning nuclear structure. Recently, magic numbers in the neutron-rich region were extensively studied, both experimentally and theoretically. For example, the disappearance of the $N = 20$ closed shell was shown in ^{32}Mg experimentally in terms of a low-lying 2^+ level [4] and a large $B(E2; 0_1^+ \rightarrow 2_1^+)$ value [5]. Also, mixing of $2s_{1/2}$ and $1p_{1/2}$ orbitals eliminates the $N = 8$ magic number in neutron-rich Li and Be isotopes [6,7]. Although the disappearance of magic numbers has been discussed, as shown above, no appearance of a magic number has thus far been shown experimentally.

In this Letter, we survey S_n and σ_I for the neutron-rich *p-sd* and the *sd* shell region to investigate a new magic number. $N = 16$ for nuclei near the neutron drip line shows a new magic number in the systematics of a neutron-number dependence of S_n and σ_I.

We show a neutron (N) number dependence of experimentally observed S_n [2] for nuclei with odd N and even Z (odd N and odd Z) in Figs. 1(a) and 1(b), respectively. In Fig. 1, a magic number appears as a decrease of S_n along with an increase of N [9]. The traditional magic numbers ($N = 8$, 20) are clearly seen close to the stable nuclei as breaks in the small T_z lines. However, the break at $N = 8$ ($N = 20$) disappears at $T_z = 3/2$ ($T_z = 4$), which is also known in connection with other experimental quantities, as discussed above. On the other hand, a break in the S_n line appears at $N = 16$ for $T_z \geq 3$, as clearly shown in

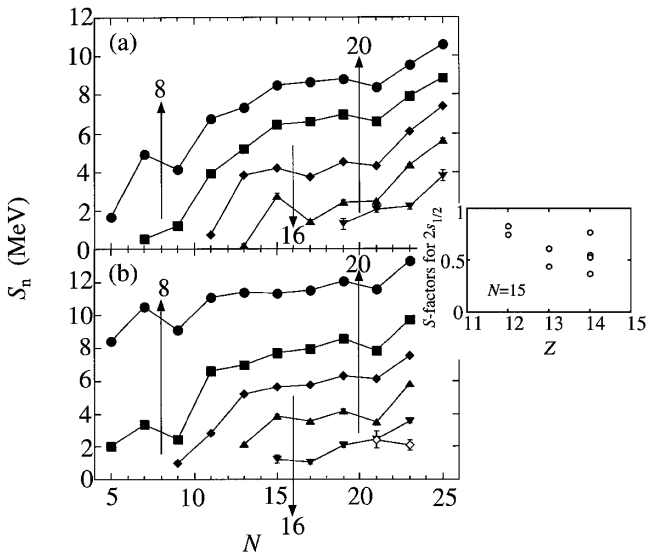

FIG. 1. (a) Neutron (N) number dependence for experimentally observed neutron separation energies (S_n) [2] for nuclei with odd N and even Z. The closed circles, closed squares, closed diamonds, closed triangles, and closed inverse triangles show different isospin numbers (T_z) from 1/2 to 9/2. (b) Neutron (N) number dependence for experimentally observed S_n [2] for nuclei with odd N and odd Z. The closed circles, closed squares, closed diamonds, closed triangles, closed inverse triangles, and open diamonds show different T_z from 0 to 5. In the figures, we do not show experimental errors below ± 10 keV. The solid lines are guides to the eye. The breaks correspond to magic numbers, as shown by arrows. The inset shows deduced spectroscopic factors (S factors) for nuclei with $N = 15$, which are data deduced from (d, p) reactions [8].

Fig. 1, which indicates the creation of a new magic number in $N = 16$ near the neutron drip line.

In Fig. 2, a neutron (N) number dependence of experimentally observed σ_I for N to Mg isotopes is shown. We observed a steep increase of σ_I from $N = 14$ to $N = 15$ for N to F isotopes, as shown in Fig. 2. On the other hand, for Ne to Mg isotopes, no steep increase of σ_I is shown in Fig. 2, although some σ_I have large error bars. It is noted that a clear difference occurs at $T_z = 3$, which suggests some correlation for the new magic number $N = 16$, as shown in S_n.

For further quantitative discussions concerning the increase of σ_I, we performed calculations similar to those in Ref. [13]. We assumed a core plus neutron structure for $N = 15$ nuclei. The density distribution for the valence neutron in a nucleus was calculated by a potential model, where single-nucleon density distributions in a core plus nucleon potential were calculated for given values of S_n. In these calculations, we assumed only $2s_{1/2}$ and $1d_{5/2}$ orbitals for the valence neutron and a Woods-Saxon shape for the potential; we also fixed the radius parameter to be $1.22A^{1/3}$ fm and the diffuseness parameter to be 0.70 fm, and adjusted the depth of the potential so as to reproduce the given S_n. The resulting single-neutron distribution was added to the core density distribution, which gave the observed σ_I for the core nucleus ($N = 14$ nuclei). For the deduced necleon density of $N = 15$ nuclei, σ_I were calculated by Glauber model calculations for few-body (FB) systems, which were developed by a Niigata group [14]. It is noted that the spectroscopic factors (S factors) deduced by the Glauber model for FB agree with those deduced by (d, p) reactions in ^{11}Be and ^{15}C [3]. A Surrey group also developed Glauber model calculations for FB [15]. They give essentially the same results as those by the Niigata group [3].

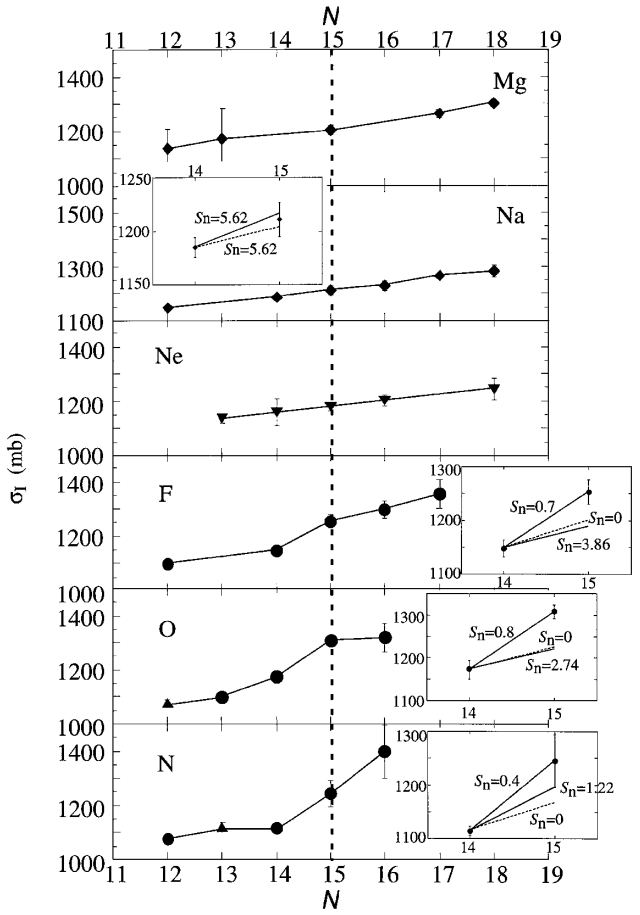

FIG. 2. Neutron (N) number dependence for the experimentally observed interaction cross sections (σ_I) for N to Mg isotopes on C targets. The closed circles, closed triangles, closed inverse triangles, and closed diamonds are data from Refs. [3], [10], [11], and [12], respectively. The solid lines are guides to the eye. The dashed line shows $N = 15$. The insets show σ_I for nuclei with $N = 14, 15$ on C targets. The solid (dashed) lines show the increase of σ_I calculated by Glauber model calculations for few-body systems assuming a pure $2s_{1/2}$ ($1d_{5/2}$) orbital for the valence neutron with given neutron separation energies (S_n), respectively. The unit of S_n is given by MeV.

As can be seen in Fig. 2, the observed σ_I can be reproduced only by using the $2s_{1/2}$ orbital. For the case of the $1d_{5/2}$ orbital, we cannot reproduce the observed σ_I even if we use $S_n = 0$ MeV, as shown by the dashed lines in the insets. Thus, we conclude a dominance of the $2s_{1/2}$ orbital for the valence neutron in ^{22}N, ^{23}O, and ^{25}F. It is noted that, since S_n, which reproduce the observed σ_I, are much smaller than those experimentally observed ($S_n = 1.22 \pm 0.22$ MeV for ^{22}N, $S_n = 2.74 \pm 0.12$ MeV for ^{23}O, and $S_n = 3.86 \pm 0.10$ MeV for ^{24}F [2]), some additional effects, such as a deformation of the cores, are necessary. A detailed discussion is given in Ref. [3]. On the other hand, the increase of σ_I from ^{25}Na to ^{26}Na can be explained by a mixing of $2s_{1/2}$ and $1d_{5/2}$ orbitals, as shown in the insets of Fig. 2. Here, we calculated σ_I using the observed S_n (= 5.62 MeV [2]) for ^{26}Na. We could not perform a meaningful analysis for Ne and Mg isotopes because of the relatively large error bars for σ_I. However, rates for the increase of σ_I for the isotopes are also similar to Na isotopes, as shown in Fig. 2. Thus, we also conclude that a valence neutron for ^{25}Ne and ^{27}Mg is a mixing of the $2s$ and $1d$ orbitals.

For nuclei with $N = 15$ near the stable line, ^{27}Mg, ^{28}Al, and ^{29}Si, S factors were investigated by (d, p) reactions [8]. The angular distribution for the results shows an s-orbital structure for the nuclei. However, as shown in the inset of Fig. 1, the deduced S factors of $2s_{1/2}$ are 0.3–0.8, which show some mixing of other orbitals for the valence neutron for the nuclei. Thus, a valence neutron in the $N = 15$ chain shows the following tendency: The purity of the $2s_{1/2}$ orbital is larger when T_z is larger. This tendency is also exhibited even for $T_z < 2$, as shown in the inset of Fig. 1. It should be noted that the purity of $2s_{1/2}$ drastically increases at $T_z = 3$. This conclusion supports the creation of a new magic number at $N = 16$ near the neutron drip line, since a clear single-particle structure is suggested for $N = 15$ nuclei near the neutron drip line.

The appearance of the new magic number at $N = 16$ near the neutron drip line and the disappearance of the

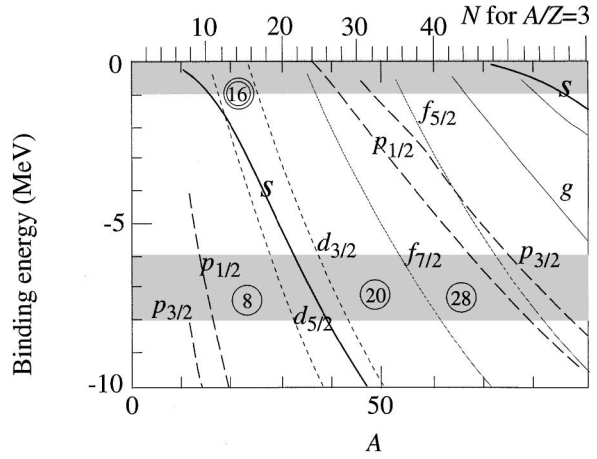

FIG. 3. Spectrum of single-neutron orbitals, obtained by the spherical Woods-Saxon potential, for $A/Z = 3$ nuclei. The lines are labeled by the single-particle orbitals. The magic numbers are indicated by the numbers inside the circles. The shaded area in the region of a binding energy of about 6–8 MeV (below 1 MeV) corresponds to that for typical stable nuclei (nuclei near the drip line), respectively.

magic number at neutron-rich $N = 20$ provides an easier view for two other recent observations: One is the nonexistence of bound "double magic" nuclei ^{28}O [16], and the other is the existence of the neutron drip line of F isotopes beyond $N = 20$ [16]. A large shell gap between $2s_{1/2}$ and $1d_{3/2}$ at neutron-rich $N = 16$ brings the $1d_{3/2}$ orbital higher up and, thus, this orbital is unbound in O isotopes (^{28}O unbound). The $1d_{3/2}$ orbital may thus be mixed with other higher orbitals. When this orbital is occupied, the many mixed higher orbitals may be close together and, thus, the drip line of F isotopes is extended.

The origin of the new magic number may be due to neutron halo formation. Figure 3 shows the single-particle orbitals of a neutron in the normal spherical Woods-Saxon potential. The single-particle orbitals were calculated for $A/Z = 3$ nuclei just to show the effect of neutron excess. Normal shell gaps $N = 8, 20, 28$ are seen in the region of a binding energy of about 6–8 MeV, as expected. However, for a weakly bound system in $A/Z = 3$ nuclei, the spacing, and even the ordering, of the orbitals changes. The most pronounced is the s orbital for $N = 9, 10$. In the region of a binding energy below 1 MeV, the $2s_{1/2}$ orbital is below the $1d_{5/2}$ orbital. This fact is clearly observed as an abnormal ground state spin parity of ^{15}C ($J^\pi = 1/2^+$). It is also observed as a strong contribution of the $2s_{1/2}$ orbital to the formation of a neutron halo in ^{11}Li, ^{11}Be, and ^{14}Be (the mixing of $(2s_{1/2})^2$ and $(1p_{1/2})^2$ in the halo wave function) [6,17]. The lowering of the s orbitals is due to halo formation. The neutron halo is formed since the orbital with a low angular momentum gains energy by extending the wave function. This effect is largest in the s orbital and next largest in the p orbital. The effect for the p orbitals is also seen in Fig. 3.

In Fig. 3, the diffuseness parameter of the Woods-Saxon potential was fixed. The lowering of the low-angular momentum orbitals is more pronounced for a potential with larger diffuseness, which is expected because of the self-consistent nature of the density distribution and the potential. Therefore, the lowering of the s orbital is expected to be more pronounced in reality.

When a neutron number increases for a weakly bound system, a strong mixing between $2s_{1/2}$ and $1d_{5/2}$ orbitals appears. Thus, the energy gap between these two orbitals and $1d_{3/2}$ becomes much larger. A weakly bound $N = 16$, the $2s_{1/2}$ and $1d_{5/2}$ orbitals are filled by neutrons leaving a large gap to the $1d_{3/2}$ orbital, as shown in Fig. 3.

Thus, the mechanism that forms a neutron halo and makes the lowering of low-angular momentum orbitals, for weakly bound neutrons, is also essential for the appearance of the magic number $N = 16$ near the neutron drip line. This mechanism may be common in nuclei near the neutron drip line. It therefore may destroy or produce other magic numbers in heavier elements also.

In summary, we have surveyed the neutron separation energies (S_n) and the interaction cross sections (σ_I) for the neutron-rich p-sd and the sd shell region. A neutron (N) number dependence of S_n shows clear breaks at $N = 16$ near the neutron drip line ($T_z \geq 3$). A neutron (N) number dependence of σ_I shows a large increase in $N = 15$ nuclei ($T_z \geq 3$), which shows that the purity of the $2s_{1/2}$ orbital is larger when T_z is larger in our analysis. These two facts indicate the appearance of a new magic number at $N = 16$ near the drip line ($T_z \geq 3$). The origin of the new magic number may be due to neutron halo formation. The mechanism used to form the new magic number may be common in nuclei near the neutron drip line. To confirm the magic number experimentally, other experimental observations, such as excited energies of the 2^+ states for $N = 16$ nuclei, are urged.

We would like to thank K. Sümmerer and L. Chulkov for their valuable comments.

[1] I. Tanihata, J. Phys. G **22**, 157 (1996).
[2] G. Audi and A. H. Wapstra, Nucl. Phys. **A595**, 409 (1995).
[3] A. Ozawa *et al.* (to be published).
[4] D. Guillemaud-Mueller *et al.*, Nucl. Phys. **A426**, 37 (1984).
[5] T. Motobayashi *et al.*, Phys. Lett. B **346**, 9 (1995).
[6] H. Simon *et al.*, Phys. Rev. Lett. **83**, 496 (1999).
[7] H. Keller *et al.*, Z. Phys. A **348**, 61 (1994).
[8] P. M. Endt, Nucl. Phys. **A521**, 1 (1990), and references therein.
[9] A. Bohr and B. R. Mottelson, *Nuclear Structure* (Benjamin, New York, 1969), Vol. 1, p. 192.
[10] L. Chulkov *et al.*, Nucl. Phys. **A603**, 219 (1996).
[11] T. Suzuki *et al.* (to be published).
[12] T. Suzuki *et al.*, Nucl. Phys. **A630**, 661 (1998).
[13] M. M. Obuti *et al.*, Nucl. Phys. **A609**, 74 (1996).
[14] Y. Ogawa *et al.*, Nucl. Phys. **A543**, 722 (1992).
[15] J. S. Al-Khalili and J. A. Tostevin, Phys. Rev. Lett. **76**, 3903 (1996).
[16] H. Sakurai *et al.*, Phys. Lett. B **448**, 180 (1999).
[17] T. Suzuki *et al.*, Nucl. Phys. **A658**, 313 (1999).